# Temperature dependence of the energy transfer from amorphous silicon nitride to Er ions

R. Li,[1] S. Yerci,[1] and L. Dal Negro[1,2,a)]
[1]*Department of Electrical and Computer Engineering & Photonics Center, Boston University, Boston, Massachusetts 02215, USA*
[2]*Division of Materials Science and Engineering, Boston University, Brookline, Massachusetts 02446, USA*

(Received 14 May 2009; accepted 2 July 2009; published online 29 July 2009)

The 1.54 $\mu$m photoluminescence and decay time of Er-doped amorphous silicon nitride films with different Si concentrations are studied in the temperature range of 4 to 320 K. The temperature quenching of the Er emission lifetime demonstrates the presence of nonradiative trap centers due to excess Si in the films. The temperature dependence and the dynamics of the energy coupling between amorphous silicon nitride and Er ions are investigated at different temperatures using two independent methods, which demonstrate phonon-mediated energy coupling. These results can lead to the engineering of more efficient Er-doped, Si-based light sources for on-chip nanophotonics applications. © *2009 American Institute of Physics*. [DOI: 10.1063/1.3186062]

Silicon (Si)-based nanostructures have been widely studied due to their ability to efficiently transfer energy to erbium (Er) ions, resulting in three orders of magnitude larger Er excitation cross sections compared to Er-doped glasses.[1,2] As a result, Er doping of silicon nanostructures potentially provides a viable solution for the engineering of on-chip light sources at 1.54 $\mu$m monolithically integrated atop the inexpensive silicon platform. Recently, Er-doped, Si-rich nitride (Er:SRN) materials have been investigated as optical platforms for Si-based photonics.[3] Similarly to Er-doped glasses, Er:SRN show intense 1.54 $\mu$m photoluminescence (PL) with small thermal quenching[4] and are ideally suited for the fabrication of high-quality photonic structures.[5] In addition, nonresonant Er excitation by nanosecond-fast energy transfer from small (2 nm) Si nanoclusters to Er ions has been demonstrated in Er:SRN.[6]

On the other hand, millisecond-long Er emission lifetimes at 1.54 $\mu$m sensitized by nonresonant energy transfer has also been recently demonstrated, in the absence of identifiable Si nanocrystals, in Er-doped, Si-rich oxide[7] and amorphous silicon nitride ($Er:SiN_x$) materials fabricated by reactive cosputtering.[8] The temperature dependence of this energy transfer mechanism has not been investigated, and needs to be understood in order to engineer efficient light-emitting devices in $Er:SiN_x$.

The temperature quenching of the sensitized Er PL intensity ($I_{PL}$) in $Er:SiN_x$ can be attributed to an increase in the de-excitation rate of Er ions and/or to a decrease in their excitation efficiency.[9,10] The former mechanism is associated to nonradiative trapping at high temperatures and can be observed by measuring the temperature dependence of the Er PL lifetime ($\tau_{PL}$). On the other hand, the latter mechanism is coupled to the temperature-dependent de-excitation rate of the sensitizing $SiN_x$ matrix. As a result, the 1.54 $\mu$m thermal quenching of the PL intensity must be studied by measuring the temperature dependence of both $I_{PL}$ and $\tau_{PL}$ along with the PL from the $SiN_x$ sensitizing matrix.

In this paper, by studying the temperature dependence of $I_{PL}$ and $\tau_{PL}$ at both the Er and the $SiN_x$ emission bands (1.54 $\mu$m and in the 0.5–0.8 $\mu$m range depending on refractive index), we investigate the nature of temperature quenching and determine the temperature dependence of the coupling parameter $\gamma$ between Er ions and the $SiN_x$.

Amorphous $Er:SiN_x$ samples were fabricated by reactive magnetron sputtering using Si and Er targets. The stoichiometry of the samples was controlled by changing $N_2/Ar$ gas flow ratio. Rapid thermal annealing was performed at temperatures between 700 and 1150 °C for 200 s to obtain the maximum Er PL intensity for samples with different excess Si. The structural properties of these materials are discussed elsewhere and no Si nanocrystals were observed in high resolution transmission electron microscopy images.[8] The refractive indices of $Er:SiN_x$, directly correlated with the amount of excess Si in the films,[8] were obtained by spectroscopic ellipsometry (A. J. Woollam VASE). The $I_{PL}$ and $\tau_{PL}$ measurements were performed between 4 and 320 K. $Er:SiN_x$ samples were excited using an Ar line at 458 nm which is nonresonant with Er absorption. The excitation laser beam was modulated by a mechanical chopper. Er $I_{PL}$ and $\tau_{PL}$ were measured by an InGaAs detector (Oriel 70368) coupled to an oscilloscope. The PL spectra of the $SiN_x$ matrices were also measured under the identical excitation conditions using a photomultiplier tube (Oriel 77348). The PL decay traces of the $SiN_x$ matrices were excited by the second harmonic of a 100 fs pulsed Ti:sapphire laser (Mai Tai HP, Spectra Physics) at 430 nm and measured by a double grating spectrometer (Acton Spectra Pro. 2300i) coupled to a streak camera with 10 ps time resolution (Hamamatsu, C4770).

Figure 1(a) shows the temperature dependence of the Er-integrated $I_{PL}$ for $Er:SiN_x$ samples with three different refractive indices in an Arrhenius plot. The $I_{PL}$ of the samples are normalized to their values at 10 K. These samples have refractive indices of 2.03 (stoichiometric $Si_3N_4$), 2.08, and 2.25 at 1.54 $\mu$m with excess Si varying from 0% to 6%.[8] We show in Fig. 1(a) that although the integrated $I_{PL}$ drops from 4 K to room temperature (RT) by approximately the same amount for all the samples [Fig.

a)Author to whom correspondence should be addressed. Electronic mail: dalnegro@bu.edu.

 © 2009 American Institute of Physics

Downloaded 26 Feb 2013 to 18.113.6.182. Redistribution subject to AIP license or copyright; see http://apl.aip.org/about/rights_and_permissions

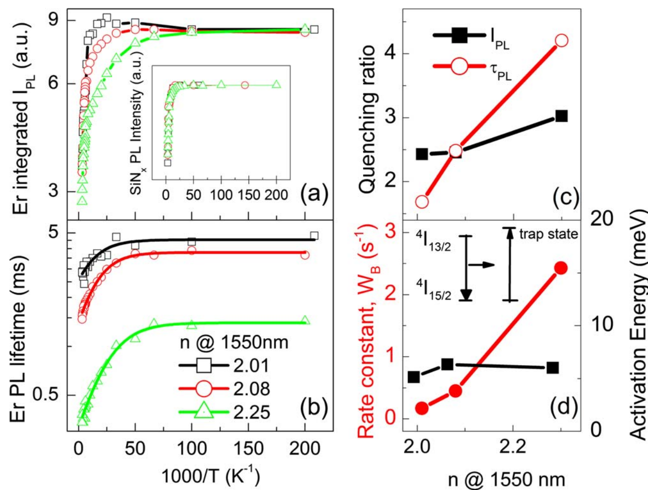

FIG. 1. (Color online) The temperature dependence of (a) Er PL intensity normalized to the value at 10 K, (b) Er PL lifetime at 1.54 $\mu$m, (c) the temperature quenching ratio of Er PL intensity (square) and lifetime (circle) at 1.54 $\mu$m between 4 K and RT, and (d) the rate constant $W_B$ (circle) and activation energy $E_A$ (triangle) as a function of refractive index. The inset of (a) is temperature dependence of $SiN_x$ integrated PL for the three samples. The inset of (d) shows a schematic energy diagram for temperature quenching of Er lifetime.

1(c)], the quenching of the integrated $I_{PL}$ begins at lower temperatures for samples with higher refractive indices. The inset of Fig. 1(a) shows that the temperature dependence of the normalized integrated PL intensities of the $SiN_x$ matrices for the three samples share the same behavior, which is consistent with previous studies and attributed to the thermal ionization from localized states.[11]

In Fig. 1(b) we show the temperature dependence of the $\tau_{PL}$ for our samples. The samples with refractive indices 2.03, 2.08, and 2.25 have $\tau_{PL}$ of 4.42, 3.90, and 1.34 ms at 4 K, respectively. These values decrease to 2.69, 1.47, and 0.34 ms at RT. The shorter $\tau_{PL}$ at 4 K is observed for the samples with the higher refractive indices, indicating the presence of nonradiative centers for Er at any temperature in the $SiN_x$ matrix. Figure 1(c) shows the temperature quenching ratios of the integrated $I_{PL}$ and $\tau_{PL}$ between 4 K and RT. We notice that the quenching ratio of $I_{PL}$ can be either larger or smaller than the quenching ratio of $\tau_{PL}$ depending on the refractive index in the sample. Therefore, the thermal quenching of $I_{PL}$ and $\tau_{PL}$ in $SiN_x$ cannot be explained by only one mechanism for samples with different stoichiometry.

As shown in Fig. 1(c), the quenching ratio of $\tau_{PL}$ is larger for samples with higher refractive index suggesting that nonradiative de-excitation paths for the $^4I_{13/2}$ $Er^{3+}$ transition are increased by the excess Si in the matrix. The Er lifetime data were fitted in Fig. 1(b) to the model $\tau = 1/[W_{r=0} + W_B \exp(-E_A/kT)]$,[12–14] where $W_{T=0}$ is the decay rate at $T=0$, $E_A$ is the activation energy of nonradiative trap states, and $W_B$ is the rate constant of the trap. This model describes the temperature dependence of the Er lifetime due to the energy transfer from Er ions to higher energy trap states distributed in the host matrix. Figure 1(d) shows the dependence of $E_A$ and $W_B$ on the refractive index of the samples. From the best fit with the model, $E_A$ varies only slightly between 5 and 6 meV while $W_B$ changes markedly with increasing refractive index. These data demonstrate the existence of nonradiative trap states separated by 5–6 meV from the Er $^4I_{13/2}$ excited level for all excess Si concentrations as shown in the inset of Fig. 1(d). Furthermore, the concentration of the trap states increases with excess Si in the samples, explaining the more significant thermal quenching of $\tau_{PL}$ for samples with higher Si concentration. Interestingly, we also found that the presence of excess Si in Er:$SiN_x$ drastically increases the nonresonant excitation cross section $\sigma_{exc}$ of Er ions at 458 nm as reported elsewhere.[8]

Additionally, the temperature dependence of the $\sigma_{exc}$ was obtained by the ratio $I_{PL}(T)/\tau(T) \sim \sigma_{exc}(T)\phi[N_{Er}]/\tau_r$, where $\phi$ is the photon flux, $[N_{Er}]$ the optically active Er concentration and $\tau_r$ the Er radiative lifetime. Assuming that $\tau_r$ and $[N_{Er}]$ are temperature independent, we see that $I_{PL}(T)/\tau_{PL}(T)$ as a function of temperature is directly proportional to $\sigma_{exc}(T)$. In Fig. 2(a), we show the temperature dependence of $\sigma_{exc}(T)$ and we observe that it increases with temperature below $\sim$150 K, while it starts decreasing at higher temperatures. This behavior has been observed in all samples, irrespective of the Si concentration.

Under steady-state and weak excitation conditions, the $\sigma_{exc}(T)$ can be expressed as (Ref. 6) $\sigma_{exc} = \sigma_{Er} + n_b(\phi, T)\gamma(T)/\phi$, where $\sigma_{Er}$ is the excitation cross section of Er by direct absorption, $\phi_p$ is the photon flux, $n_b$ is the excited state population of the sensitizer (the $SiN_x$ matrix), and $\gamma$ is the fundamental coupling coefficient between the sensitizer and Er. In order to extract the temperature dependence of $\gamma$, we measured the PL intensity from $SiN_x$ matrix at different temperatures.

Figure 2(a) shows the temperature dependence of both $\sigma_{exc}(T)$ and the PL intensity of the $SiN_x$ sample with refractive index 2.25. The PL intensity is directly proportional to

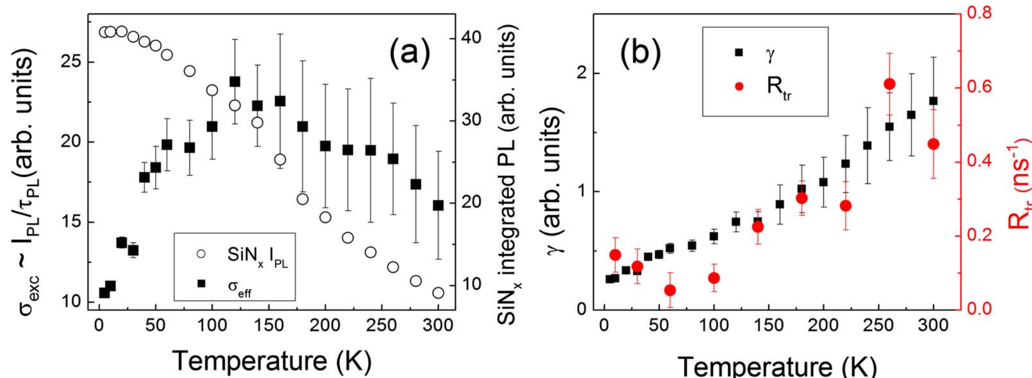

FIG. 2. (Color online) (a) Temperature dependence of $I_{PL}/\tau_{PL}$ (square) in the sample with refractive 2.25 and $SiN_x$ integrated PL intensity (circle). (b) Coupling coefficient $\gamma$ (square) and transfer rate $R_{tr}$ (circle) between $SiN_x$ and Er.

Downloaded 26 Feb 2013 to 18.113.6.182. Redistribution subject to AIP license or copyright; see http://apl.aip.org/about/rights_and_permissions

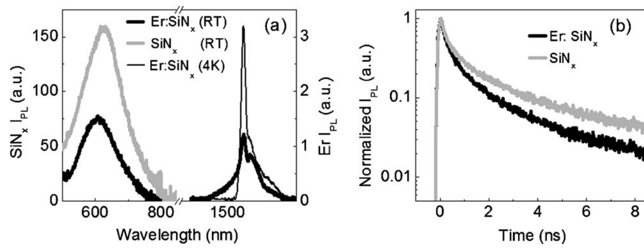


FIG. 3. (a) Visible PL spectrum at RT for $SiN_x$ samples doped and undoped with Er together with Er PL spectra at RT and 4 K. (b) PL lifetime at 600 nm from $SiN_x$ matrix.

the excited state population of the sensitizer $n_b(T)$. Therefore, $\sigma_{exc}(T)/n_b(T)$ gives us the temperature dependence of $\gamma(T)$, which is shown in Fig. 2(b).

While $\gamma(T)$ is obtained from the excitation of Er, the transfer rate $R_{tr}(T)$ can also be obtained from the deexcitation of the sensitizing $SiN_x$ matrix by time-resolved PL decay measurements. In order to investigate the dynamics of energy transfer, we fabricated a pair of $SiN_x$ samples containing the same excess Si ($n \sim 2.03$) doped (Er:$SiN_x$) and undoped ($SiN_x$) with Er. The $SiN_x$ visible emission and Er $I_{PL}$ spectra at 300 K for doped and undoped samples are shown in Fig. 3(a). In addition, the Er PL spectrum measured at 4 K is also shown to demonstrate the overall Er PL quenching. The sizeable reduction of the Er emission line shape at 4 K is expected for phonon-coupled inhomogeneously broadened transitions.[15] The PL decay traces of the samples measured in the visible spectral range are shown in Fig. 3(b). The reduction in the visible PL intensity and shortening of the visible lifetime for the Er doped sample are due to the energy transfer from $SiN_x$ to the Er ions, considering the low Er concentration ($\sim 0.37\%$).[6,8,16] The transfer rate $R_{tr}$ can be estimated at any temperature, under weak pumping conditions, by $1/\tau_d = 1/\tau_{ud} + R_{tr}$ where $\tau_d$ and $\tau_{ud}$ are the measured PL decay times for Er doped and undoped $SiN_x$.[3,16] The PL decay traces, measured at 600 nm, of the two samples were fitted using three exponential decays convoluted with the system response. The longest component was used in the calculation since it dominates the PL intensity under continuous wave excitation. Following this procedure, we obtained $R_{tr}$ equal to 0.054 $ns^{-1}$ which corresponds to a transfer time of 18 ns at RT at 300 K.

The temperature dependent energy transfer rate $R_{tr}(T)$ for the sample with $n \sim 2.25$ measured by time-resolved measurements is plotted along with $\gamma(T)$ in Fig. 2(b). $R_{tr}(T)$ and $\gamma(T)$ share the same temperature dependence, since $R_{tr}(T)$ is equal to the product of $\gamma(T)$ and $[N_{Er}]$, where $[N_{Er}]$ is independent on temperature. The temperature dependence of $R_{tr}(T)$ and $\gamma(T)$, investigated by two independent experimental methods, consistently indicates a sevenfold enhancement of the energy transfer between $SiN_x$ and Er at high temperatures due to phonon-mediated energy transfer.[17] As a result, the temperature dependence of $\sigma_{exc}(T)$ shown in Fig. 2(a) originates from the competition between the increase in the energy transfer rate and the decrease of the excited state density of sensitizer centers with temperature. The strong temperature dependence of the energy transfer suggests the possibility of thermally assisted tunneling of photoexcited carriers from localized states in the band tails of the amorphous $SiN_x$ matrix to the location of Er ions, which can be subsequently excited by short-range coupling.[18] The high density of band-tail states could account for the nanosecond-fast energy transfer time in Er:$SiN_x$.

In conclusion, we measured the temperature dependence of Er $^4I_{13/2}$, $I_{PL}$, and $\tau_{PL}$ in Er:$SiN_x$ for different Si concentrations. We showed that excess Si enhances the excitation efficiency of Er at the expenses of its PL efficiency. Finally, we measured by two independent methods the temperature dependence of the fundamental coupling coefficient $\gamma$ between the $SiN_x$ and Er and we demonstrated that it strongly increases with temperature. Based on these data, we proposed that energy transfer in Er:$SiN_x$ could originate from phonon-assisted tunneling of carriers trapped at localized states within the band tails of the material.

This project was funded by the AFOSR under MURI Award No. FA9550-06-1-0470.

[1] M. Fujii, M. Yoshida, Y. Kanzawa, S. Hayashi, and K. Yamamoto, Appl. Phys. Lett. **71**, 1198 (1997).
[2] D. Pacifici, G. Franzò, F. Priolo, F. Iacona, and L. Dal Negro, Phys. Rev. B **67**, 245301 (2003).
[3] L. Dal Negro, R. Li, J. Warga, and S. N. Basu, Appl. Phys. Lett. **92**, 181105 (2008).
[4] N. M. Park, T. Kim, S. Kim, G. Sung, B. Kim, K. Cho, J. H. Shin, B. Kim, S. Park, J. Lee, and M. Nastasi, Thin Solid Films **475**, 231 (2005).
[5] M. Makarova, V. Sih, J. Warga, R. Li, L. Dal Negro, and J. Vuckovic, Appl. Phys. Lett. **92**, 161107 (2008).
[6] L. Dal Negro, R. Li, J. Warga, S. Yerci, S. Basu, S. Hamel, and G. Galli, in *Silicon Nanophotonics: Basic Principles, Present Status and Perspectives*, edited by L. Khriachtchev (World Scientific, Singapore, 2008).
[7] O. Savchyn, R. M. Todi, K. R. Coffey, and P. Kik, Appl. Phys. Lett. **93**, 233120 (2008).
[8] S. Yerci, R. Li, S. O. Kucheyev, T. Van Buuren, S. N. Basu, and L. Dal Negro, Appl. Phys. Lett. **95**, 031107 (2009).
[9] W. Fuhs, I. Ulber, G. Weiser, M. S. Bresler, O. B. Gusev, A. N. Kuznetsov, V. Kh. Kudoyarova, E. I. Terukov, and I. N. Yassievich, Phys. Rev. B **56**, 9545 (1997).
[10] M. J. Kim, G. K. Mebratu, and J. H. Shin, J. Non-Cryst. Solids **332**, 53 (2003).
[11] L. Dal Negro, J. H. Yi, J. Michel, L. C. Kimerling, T.-W. F. Chang, V. Sukhovatkin, and E. H. Sargent, Appl. Phys. Lett. **88**, 233109 (2006).
[12] J. I. Pankove, *Optical Processes in Semiconductors* (Dover, New York, 1975).
[13] F. Priolo, G. Franzò, S. Coffa, A. Polman, S. Libertino, R. Barklie, and D. Carey, J. Appl. Phys. **78**, 3874 (1995).
[14] A. Polman, J. Appl. Phys. **82**, 1 (1997).
[15] P. C. Becker, N. A. Olsson, and J. R. Simpson, *Erbium-Doped Fiber Amplifiers—Fundamentals and Technology* (Academic, San Diego, 1999), Chap. 4.
[16] R. Li, J. R. Schneck, J. Warga, L. D. Ziegler, and L. Dal Negro, Appl. Phys. Lett. **93**, 091119 (2008).
[17] I. Izeddin, D. Timmerman, T. Gregorkiewicz, A. S. Moskalenko, A. A. Prokofiev, I. N. Yassievich, and M. Fujii, Phys. Rev. B **78**, 035327 (2008).
[18] B. Garrido, C. García, P. Pellegrino, D. Navarro-Urrios, N. Daldosso, L. Pavesi, F. Gourbilleau, and R. Rizk, Appl. Phys. Lett. **89**, 163103 (2006).

Downloaded 26 Feb 2013 to 18.113.6.182. Redistribution subject to AIP license or copyright; see http://apl.aip.org/about/rights_and_permissions